Alterations in microRNA-124 and AMPA receptors contribute to social behavioral deficits in frontotemporal dementia

Eduardo Gascon, Kelleen Lynch, Hongyu Ruan, Sandra Almeida, Jamie Verheyden, William W. Seeley, Dennis W. Dickson, Leonard Petrucelli, Danqiong Sun, Jian Jiao, Hongru Zhou, Mira Jakovcevski, Schahram Akbarian, Wei-Dong Yao, Fen-Biao Gao

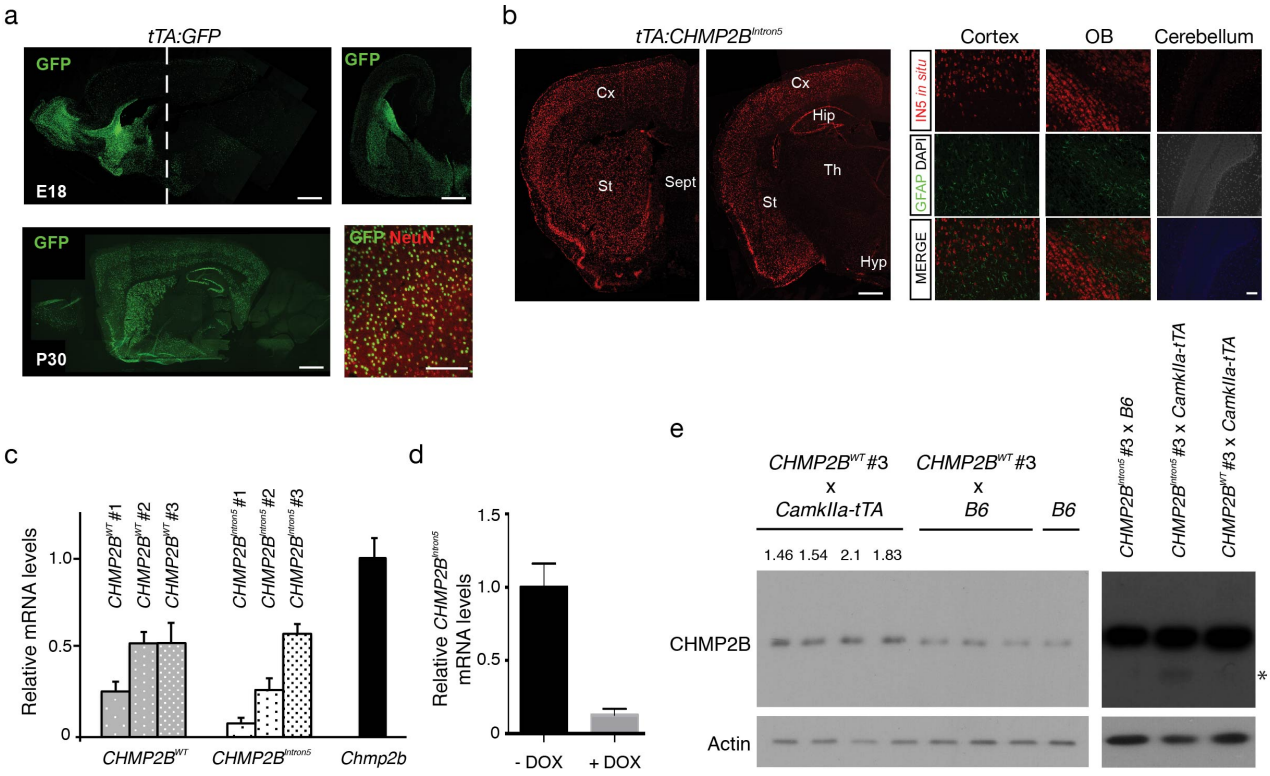

Supplementary Figure 1. Basic characterization of transgenic *tTA:CHMP2B*^{WT} and *tTA:CHMP2B*^{Intron5} mice. (**a**) GFP expression driven by *CamkIIα-tTA*. Upper panels show GFP expression in a sagittal (left) or coronal (right) brain section at E18. In the lower panel (left), a sagittal section at P30 revealed widespread expression in the cortex, striatum, olfactory bulb (OB) and hippocampus but low or no expression in other brain areas such as cerebellum or thalamus. The right lower panel shows all GFP-positive cells are neurons in the cortex of P30 mice. (**b**) Left panels show transgene expression in coronal sections of *tTA:CHMP2B*^{Intron5} mice at P30. Right panels show the absence of transgene expression in astrocytes in the cortex or olfactory bulb (OB) of *tTA:CHMP2B*^{Intron5} mice. (**c**) mRNA levels of *CHMP2B*^{WT} or *CHMP2B*^{Intron5} in the cortex of the different lines of transgenic mice (normalized to β-actin). We plotted the level of the mouse endogenous *Chmp2b* gene as reference. (**d**) *CHMP2B*^{Intron5} mRNA

levels in the cortex of mice fed a regular diet (–Dox) or a diet containing doxycycline (+Dox) for 8 months (normalized to β-actin). (**e**) Confirmation of transgene expression at the protein level by Western blot. The expression of transgenic $CHMP2B^{WT}$ (observed as an increase in the endogenous band since mChmp2b and hCHMP2B are identical except for one amino acid) and $CHMP2B^{Intron5}$ (observed as a lower band, asterisk). Since the antibody is directed against the C-terminal part of the protein (truncated in $CHMP2B^{Intron5}$), it could not be used for quantification. B6: C57BL/6. Scale bar, 200 μm in **a**, 200 μm (left panels) and 50 μm (right panels) in **b**.

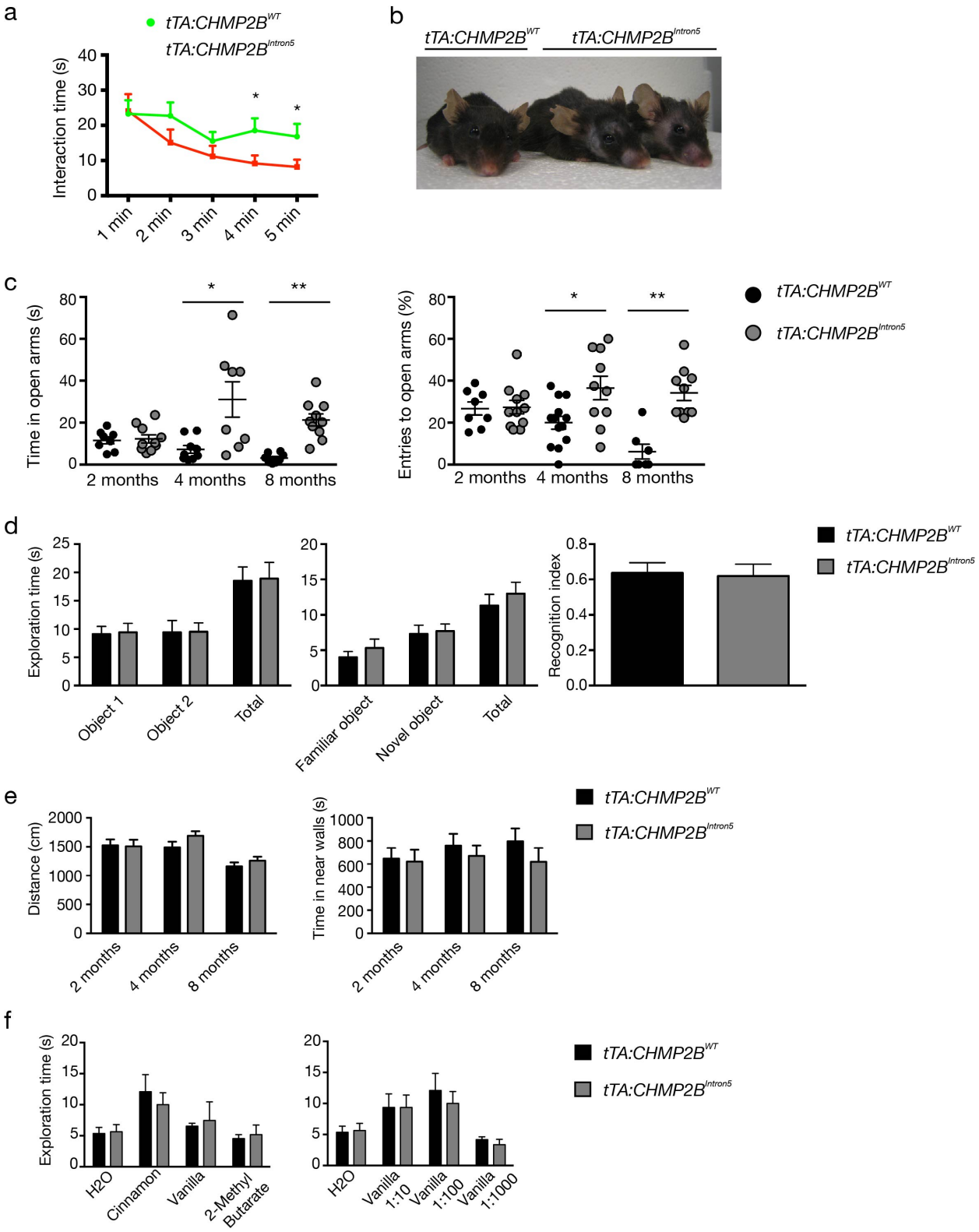
a
tTA:CHMP2B^WT
tTA:CHMP2B^Intron5
Interaction time (s)
40
30
20
10
0
1 min
2 min
3 min
4 min
5 min
*
*
b
tTA:CHMP2B^WT
tTA:CHMP2B^Intron5
c
Time in open arms (s)
80
60
40
20
0
2 months
4 months
8 months
*
**
Entries to open arms (%)
80
60
40
20
0
2 months
4 months
8 months
*
**
tTA:CHMP2B^WT
tTA:CHMP2B^Intron5
d
Exploration time (s)
25
20
15
10
5
0
Object 1
Object 2
Total
20
15
10
5
0
Familiar object
Novel object
Total
Recognition index
0.8
0.6
0.4
0.2
0.0
tTA:CHMP2B^WT
tTA:CHMP2B^Intron5
e
Distance (cm)
2000
1500
1000
500
0
2 months
4 months
8 months
Time in near walls (s)
1000
800
600
400
200
0
2 months
4 months
8 months
tTA:CHMP2B^WT
tTA:CHMP2B^Intron5
f
Exploration time (s)
20
15
10
5
0
H2O
Cinnamon
Vanilla
2-Methyl Butarate
20
15
10
5
0
H2O
Vanilla 1:10
Vanilla 1:100
Vanilla 1:1000
tTA:CHMP2B^WT
tTA:CHMP2B^Intron5

Supplementary Figure 2. Further behavioral characterization of transgenic *tTA:CHMP2B*^{WT} and *tTA:CHMP2B*^{Intron5} mice. (**a**) Interaction in home cage task in 8-month-old *tTA:CHMP2B*^{WT} and *tTA:CHMP2B*^{Intron5} mice. The difference in interaction time (defined as the time the test mouse explores the intruder mouse in 1-min intervals) is significant at the end of the task (4 min and 5 min time points. $n = 11$ mice per genotype; $P < 0.05$ at 4 min, $P < 0.05$ at 5 min by two-sided t test). (**b**) Cutaneous lesions consistent with excessive grooming are observed in a subset of individually caged *tTA:CHMP2B*^{Intron5} (two on the right) but not in *tTA:CHMP2B*^{WT} (first on the left) at old ages (14–20 months). (**c**) Time spent (left graph) and number of entries into the open arms (right graph) of the elevated plus maze (for *tTA:CHMP2B*^{WT}, $n = 8$ mice at all time points; for *tTA:CHMP2*^{Intron5}, $n = 10$ at 2 and 8 months and $n = 8$ at 4 months; time spent in open arms: $P < 0.01$ at 4 months, $P < 0.001$ at 8 months by two-sided t test; entries to open arms: $P < 0.02$ at 4 months, $P < 0.001$ at 8 months by two-sided t test). (**d**) Quantification of the time *tTA:CHMP2B*^{WT} and *tTA:CHMP2B*^{Intron5} mice at 8 months exploring the different objects presented in the novel object recognition task during the familiarization phase (left) or the test phase (middle) ($n = 10$ for *tTA:CHMP2B*^{WT} mice and $n = 11$ *tTA:CHMP2B*^{Intron5} mice, $P > 0.5$ by two-way ANOVA). Proportion of time exploring the novel object in the test phase (recognition index) is showed in the right panel. (**e**) Quantification of the distance traveled (left panel) or the time spent close to the arena walls (thigmotaxis, right panel) in the open-field task ($n = 11$ mice per genotype, $P > 0.2$ by two-sided t test). (**f**) Analysis of olfactory discrimination (left) and sensitivity (right) in *tTA:CHMP2B*^{WT} and *tTA:CHMP2B*^{Intron5} mice at 8 months ($n = 10$ mice per genotype; $P > 0.4$ by two-sided t test). All values are mean ± s.e.m.

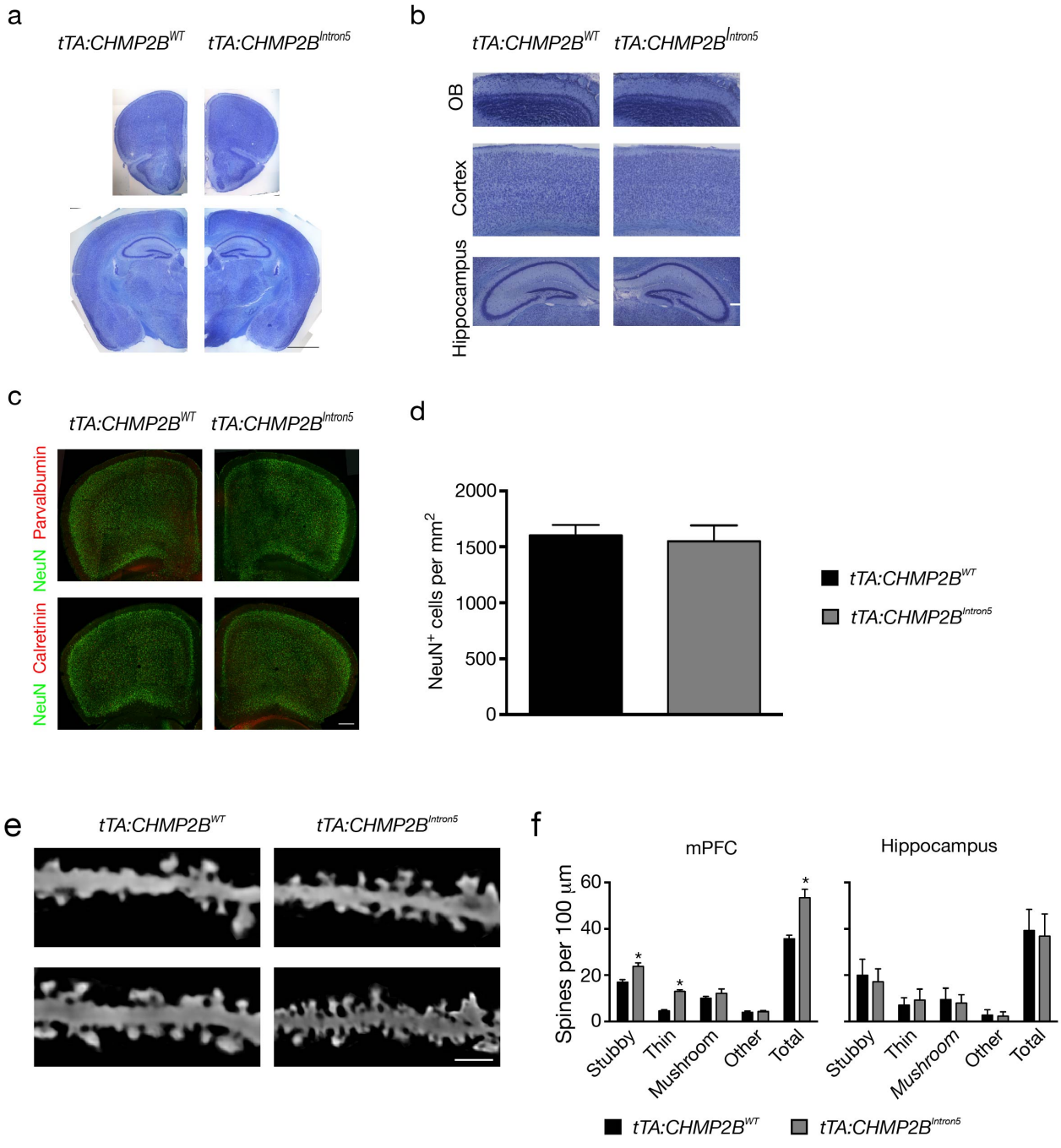

Supplementary Figure 3. Histological characterization of *tTA:CHMP2B*^{WT} and *tTA:CHMP2B*^{Intron5} mice. (**a**) Nissl-stained sections of *tTA:CHMP2B*^{WT} and *tTA:CHMP2B*^{Intron5}

mice at 8 months showing that expression of *CHMP2B*^{Intron5} leads to no overt brain defects or neuronal loss. (**b**) Higher-magnification photos of forebrain regions where the transgene was more expressed (*upper panels*, olfactory bulb; *middle panels*, cortex; *lower panels*, hippocampus) show no obvious differences between *tTA:CHMP2B*^{WT} (*left panels*) and *tTA:CHMP2B*^{Intron5} mice (*right panels*). (**c**) Immunofluorescence of neuronal markers in the rostral forebrain of *tTA:CHMP2B*^{WT} and *tTA:CHMP2B*^{Intron5} mice. In mice expressing mutant CHMP2B, we did not detect neuronal loss with a broad neuronal marker (NeuN) or an interneuron-specific marker. (**d**) NeuN density in the mPFC of *tTA:CHMP2B*^{WT} and *tTA:CHMP2B*^{Intron5} mice at 8 months (n = 4 mice per genotype; $P > 0.5$ by two-sided t test). (**e**) Representative dendritic segments of mPFC layer II-III pyramidal neurons (apical dendrite) in *tTA:CHMP2B*^{WT} and *tTA:CHMP2B*^{Intron5} mice at 8 months (Golgi staining). (**f**) *Left*: quantitative analysis of spine density and morphology of mPFC layer II-III pyramidal neurons (left) and on apical dendrites of CA3 hippocampal pyramidal neurons (right) (n = 4 mice per genotype; $P < 0.02$ for stubby spines, $P < 0.01$ for thin spines, $P < 0.001$ for total spines by two-sided two-way ANOVA corrected for multiple comparison and Bonferroni test). Scale bar, 1 mm in **a**, 300 μm in **b** and **c**, 5 μm in **e**. Values are mean ± s.e.m. in **d** and mean ± s.d. in **f**.

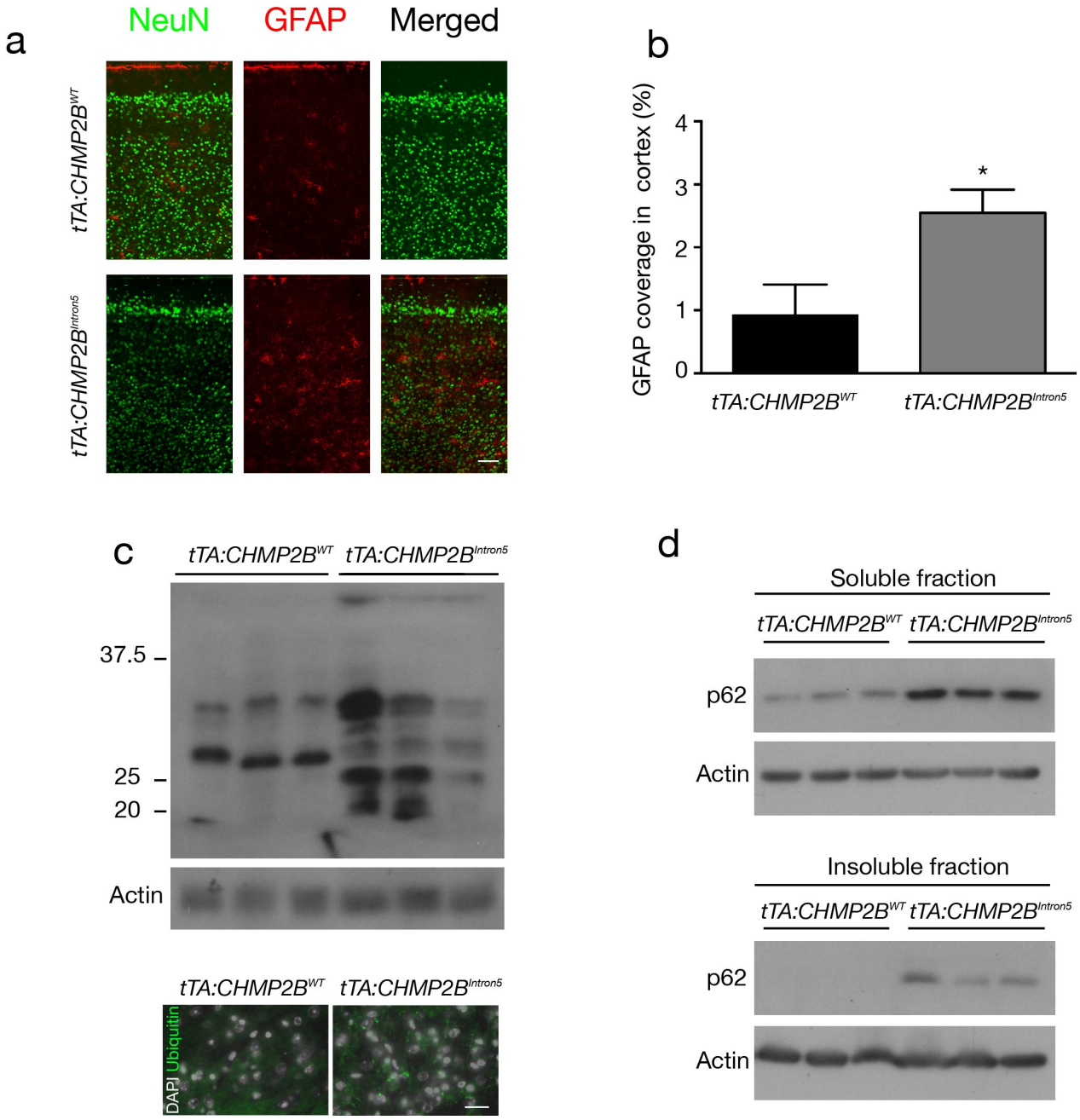

Supplementary Figure 4. Pathological phenotypes of *tTA:CHMP2B*^{Intron5} mice. (**a**) Representative photos of the mPFC of *tTA:CHMP2B*^{WT} and *tTA:CHMP2B*^{Intron5} mice at 8 months stained with GFAP (red) and NeuN (green). (**b**) GFAP coverage in the cortex of *tTA:CHMP2B*^{WT}

and *tTA:CHMP2B*^{Intron5} mice at 8 months (n = 4 mice per genotype; *: $P < 0.05$ by two-sided t test). (**c**) *Upper panel*: Western blot analysis of ubiquinated proteins in cortical samples from *tTA:CHMP2B*^{WT} and *tTA:CHMP2B*^{Intron5} mice at 12 months. Ubiquitinated species were modestly increased in *tTA:CHMP2B*^{Intron5} mice. *Lower panels*: immunofluorescence staining with an anti-ubiquitin antibody revealed a limited amount of protein deposits in the cells. (**d**) Western blot analysis of p62 expression in cortical samples of *tTA:CHMP2B*^{WT} and *tTA:CHMP2B*^{Intron5} mice at 12 months. p62 was upregulated in both soluble and insoluble fractions from mutant mice. Scale bar, 50 μm in (**a**) and 20 μm in (**c**).

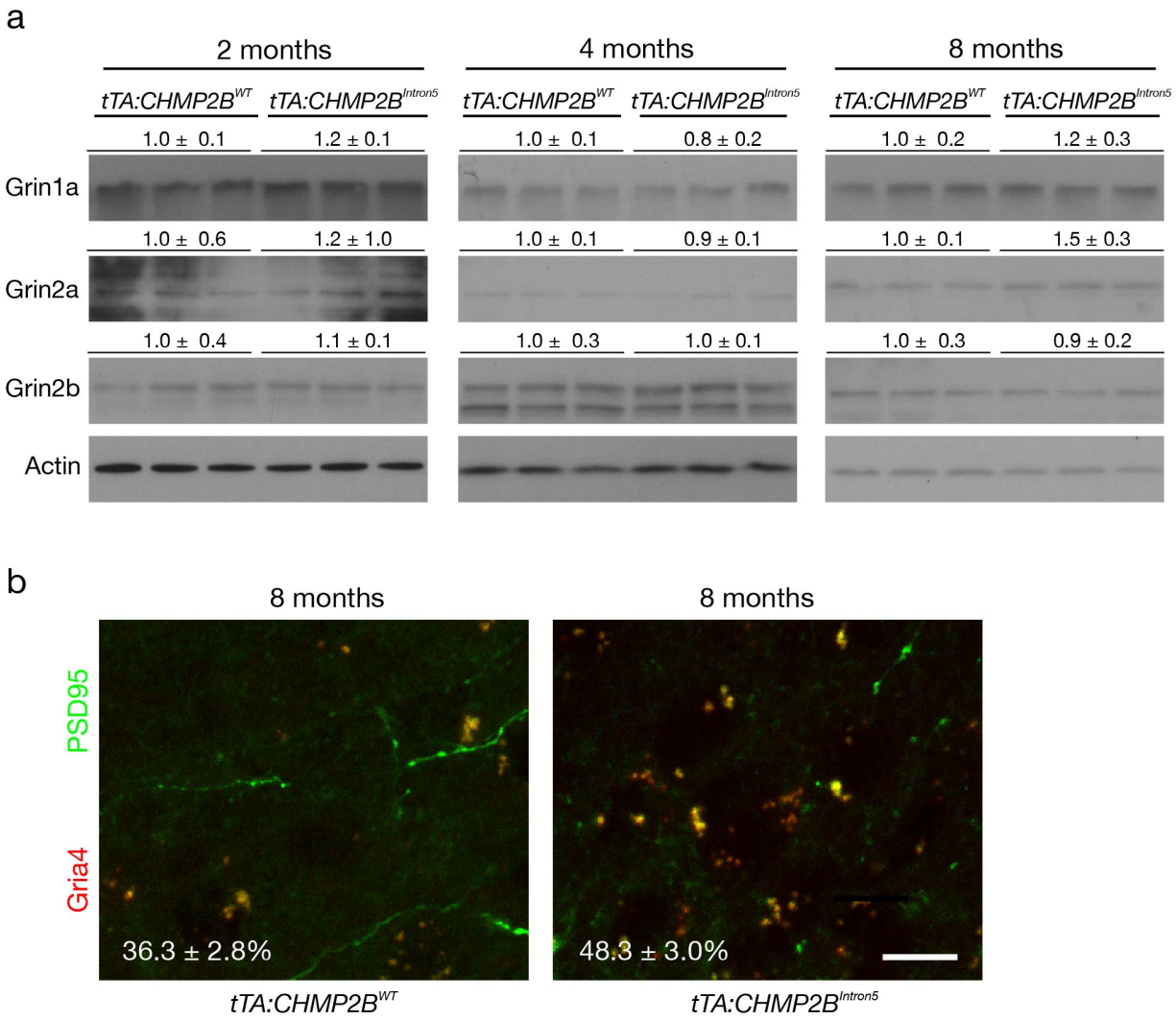

Supplementary Figure 5. Further characterization of glutamate receptors in *tTA:CHMP2B*^{Intron5} mice. (**a**) Representative western blots of PSD fractions of *tTA:CHMP2B*^{WT} and *tTA:CHMP2B*^{Intron5} mice (2, 4, and 8 months) probed with anti-Grin1 (*upper panels*), anti-Grin2a (*middle panels*), and anti-Grin2b (*lower panels*). (**b**) Quantification of the percentage of Gria4-positive puncta among all PSD95-positive puncta after double immunostaining for PSD95 (green) and Gria4 (red) in the mPFC of 8-month-old *tTA:CHMP2B*^{WT} and *tTA:CHMP2B*^{Intron5} mice ($P < 0.01$). Scale bar, 200 μm.

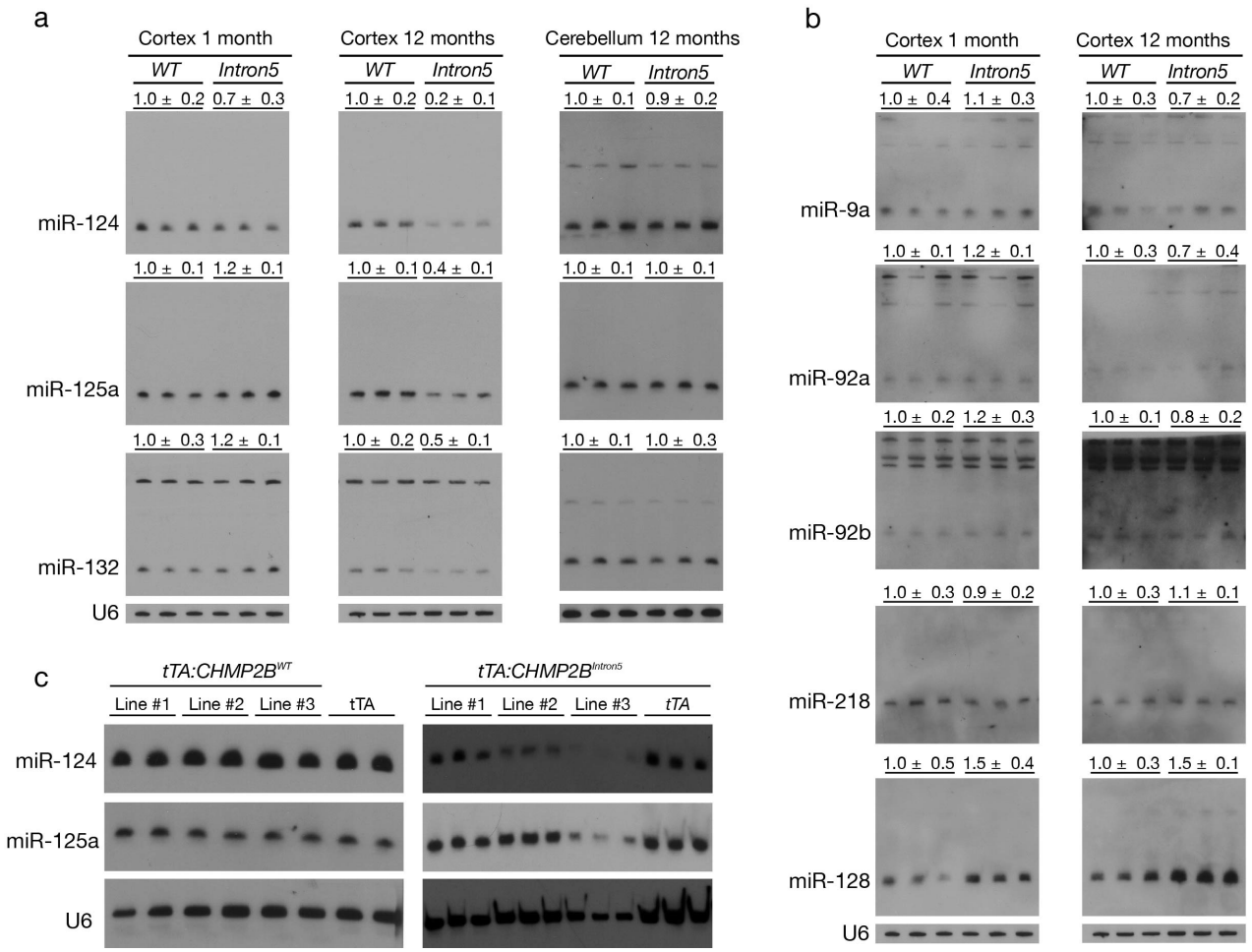

Supplementary Figure 6. Time-dependent changes in other miRNAs in *tTA:CHMP2B*^{WT} and *tTA:CHMP2B*^{Intron5} cortex. (**a**) Northern blot analysis of miR-124, miR-125a and miR-132, in cortical samples at 1 month and 12 months of age. As control, we extracted RNA from the cerebellum of *tTA:CHMP2B*^{WT} and *tTA:CHMP2B*^{Intron5} mice (age 12 months) and also probed for those miRNAs. (**b**) Northern blot analysis of miR-9, miR-92a, miR-92b, miR-134, miR-218, and miR-128 in cortical samples of *tTA:CHMP2B*^{WT} and *tTA:CHMP2B*^{Intron5} mice at 1 month and 12 months of age. (**c**) Northern blot analysis of miR-124 and miR-125a in cortical samples at 12 months of age in different lines of *tTA:CHMP2B*^{WT} (*left*) and *tTA:CHMP2B*^{Intron5} mice (*right*).

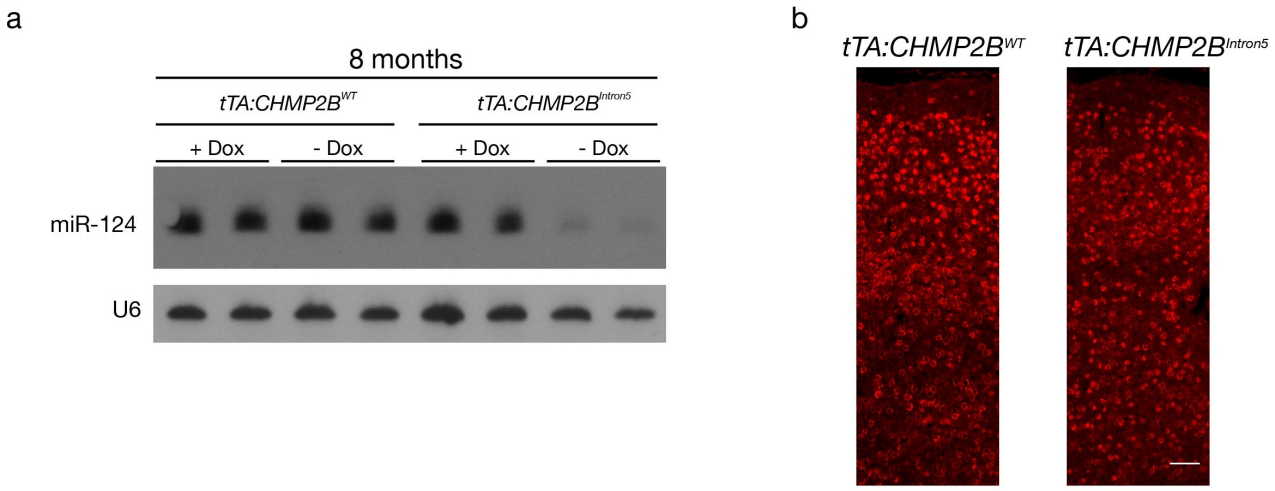

Supplementary Figure 7. miR-124 downregulation is a consequence of CHMP2B^{Intron5} expression. (**a**) Northern blot of miR-124 levels in the cortex of *tTA:CHMP2B^{WT}* and *tTA:CHMP2B^{Intron5}* mice fed with regular or doxycycline-containing food from embryonic development to 8 months. RNA in each lane was isolated from one animal. (**b**) Fluorescence *in situ* analysis of miR-124 showed its similar neuronal expression in the cortex of *tTA:CHMP2B^{WT}* and *tTA:CHMP2B^{Intron5}* mice (2 months old). Scale bar, 20 μm.

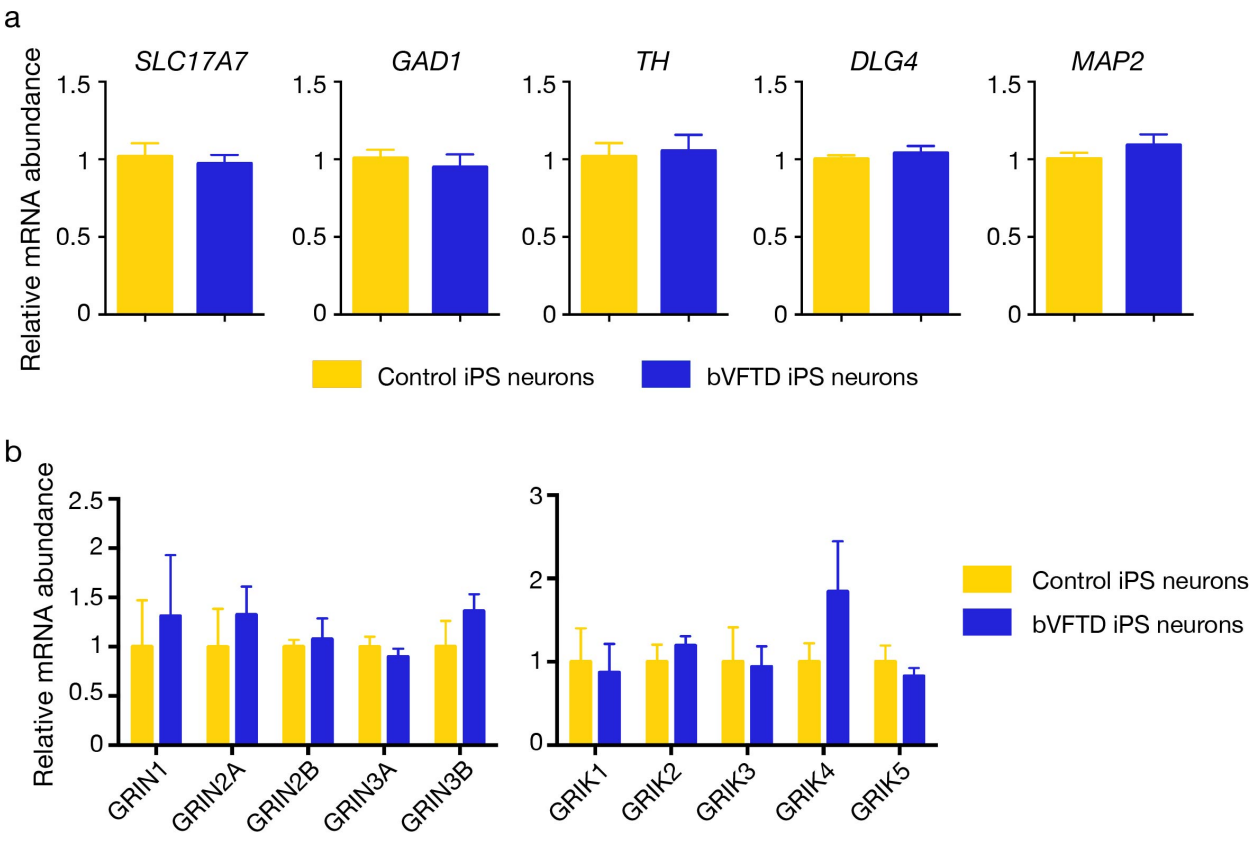

Supplementary Figure 8. Neuronal differentiation from iPSC lines. (**a**) Quantification of mRNA levels for different neuronal subtype-specific markers, such as vGLUT1 for excitatory neurons (encoded by *SLC17A7*), GAD67 for inhibitory neurons (encoded by *GAD1*), TH for dopaminergic neurons, as well as general neuron-specific markers such as PSD95 (encoded by DLG4) and MAP2 in 8-week-old neurons differentiated from 4 iPSC lines used in Figure 5. (**b**) Expression levels of kainate and NMDA subunits in 8-week-old neurons differentiated from 4 iPSC lines. $P > 0.5$ by two sided *t* test.

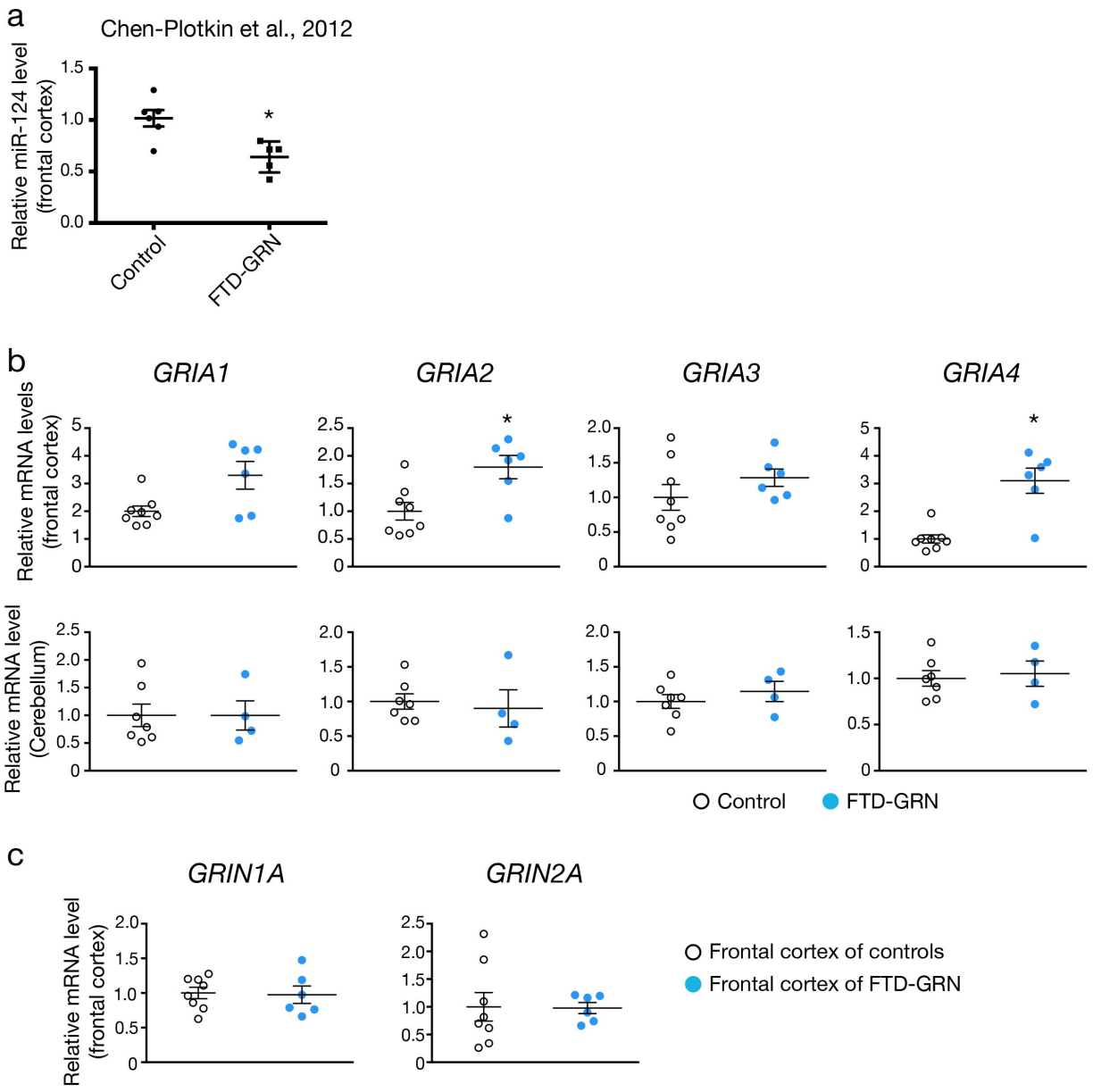

Supplementary Figure 9. Dysregulation of miR-124 and AMPARs specifically in the frontal cortex of a subset of FTD cases. (**a**) Re-analysis of miR-124 level in the frontal cortex of FTD brains from previously published profiling data[38]. In this study, $n = 6$ for controls and $n = 5$ for FTD-GRN; *: $P < 0.05$ by Mann-Whitney test. (**b**) Re-analysis of *GRIA2* and *GRIA4* in the

frontal cortex and the cerebellum of subjects with FTD-GRN, based on published data from a microarray study[39]. To compensate for any potential neuronal loss in FTD brains, we normalized AMPARs mRNAs contents against the geometric mean of four different neuronal-specific reference genes (MAP2, Enolase 2, GAP43 and PSD95). Cortex samples: $n = 8$ for controls, $n = 6$ for FTD-GRN; cerebellum samples: $n = 7$ for controls, $n = 4$ for FTD-GRN; *: $P < 0.05$; **: $P < 0.01$ by Mann-Whitney test. (**c**) Re-analysis of mRNAs encoding NMDA receptor subunits 1 and 2a using the same published dataset[39] (*: $P > 0.5$ by Mann-Whitney test). Values are mean ± s.e.m.

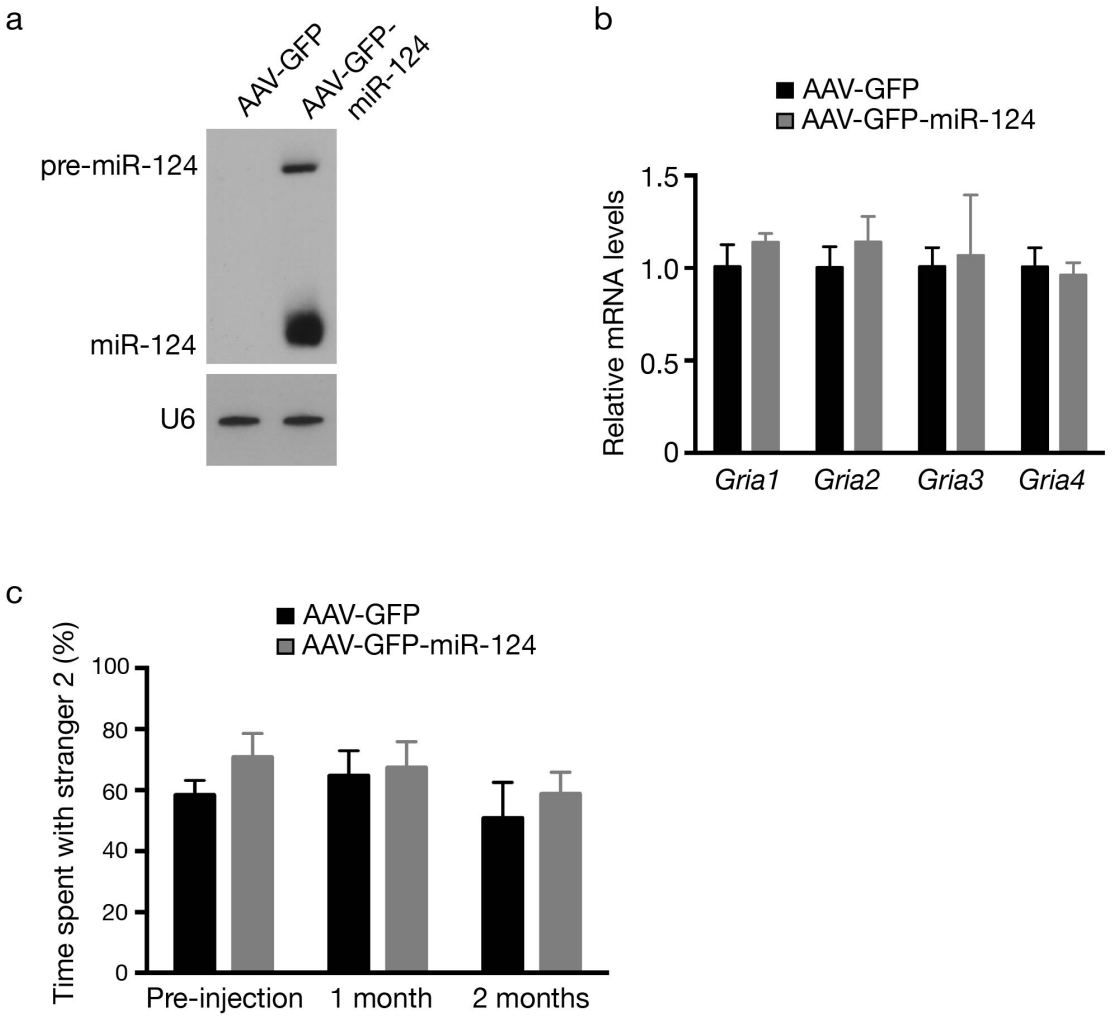

Supplementary Figure 10. Some effects of miR-124 rescue. (**a**) Northern blot analysis of the efficiency of the AAV-GFP-miR124 construct in driving miR-124 expression in HEK cells. (**b**) qRT-PCR analysis of Gria transcripts in the occipital cortex *tTA:CHMP2B*^{Intron5} mice 2 months after AAV injection in the mPFC (n = 5 AAV-GFP-infected mice and n = 4 AAV-GFP-miR-124-infected mice; $P > 0.2$ by two-sided t test). (**c**) Analysis of Social memory and novelty after AAV-mediated delivery of miR-124. At all time points, the proportion of time spent with

Stranger 2 was similar in *tTA:CHMP2B*^{Intron5} mice injected with AAV-GFP and those injected with AAV-GFP-miR-124 (n = 10 per AAV vector; $P > 0.3$ by two-sided repeated-measures two-way ANOVA corrected for multiple comparison, Bonferroni test. Values are mean ± s.d. in **b** and mean ± s.e.m. in **c**.

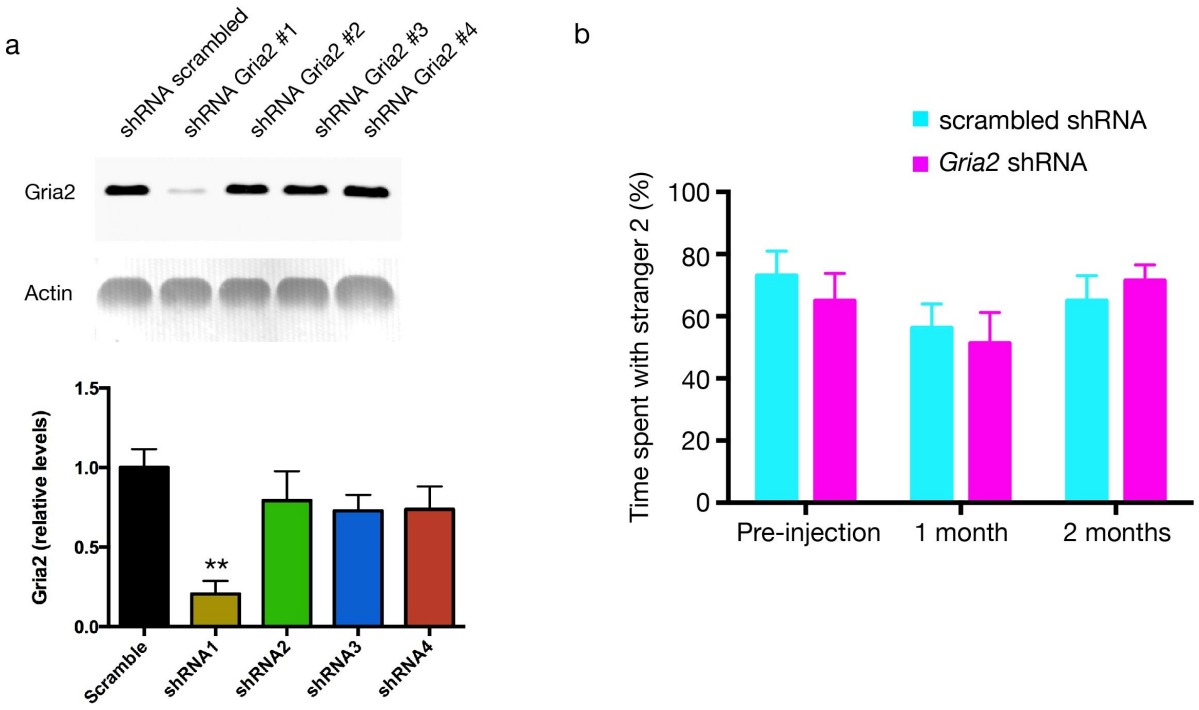

Supplementary Figure 11. The effects of *Gria2* knockdown. (**a**) *In vitro* efficiency of four different shRNAs targeting *Gria2* in mouse cortical cultures 72 h after infection with lentiviral vectors expressing GFP and either a scrambled shRNA or an shRNA against mouse *Gria2*. *Lower panel* shows the quantification of 3 independent experiments (**: $P < 0.01$ one-way ANOVA followed by Bonferroni's test). (**b**) Analysis of social memory after *Gria2* knockdown in *tTA:CHMP2B*^{Intron5} mice ($n = 7$ per genotype; $P > 0.4$ by two-sided repeated-measures two-way ANOVA followed by Fisher's least-significant-difference test). Values are mean ± s.e.m.

Supplementary Table 1. Neurotransmitter receptors whose mRNAs are targeted by miR-124 in mouse and human.

Receptor	Number of subunits	Potential miR-124 targets
GABA	16	0
Nicotinic (acetylcholine)	17	0
Muscarinic (acetylcholine)	5	0
Dopamine	5	0
Adrenergic	4	0
Serotonin	15	1
Glycine	5	1
Glutamate		
Metabotropic	8	0
Kainate	5	0
NMDA	7	1
AMPA	4	3

Supplementary Table 2. Primers used in this study.

Genes	Primer Sequences	Product Sizes (bp)
CHMP2B^{Intron5}	Forward TGACGGTTCTGATGACGAAGAAG Reverse GGGAGGGTGTGGGAGGTTTT	146
CHMP2B	Forward AAAGTGATGAATTCCCAAATGAA Reverse TCTTGTTAACTGCCTGCATTGT	76
Chmp2b	Forward GGACCGAGCAGCCTTAGAG Reverse CCAATCTTGGCCATCTTCTTA	69
Pri-miR-124-1	Forward TTCTCCCATCCTCCCTCTCT Reverse AATCAAGGTCCGCTGTGAAC	144
Pri-miR-124-2	Forward GTTCACAGCGGACCTTGATT Reverse TCTCCCCACCCTTCCTAACT	116
Pri-miR-124-3	Forward CGGTGAATGCCAAGAGAGG Reverse ATTGTTCGCCGGATTTGTC	147
mGria1	Forward AGGGATCGACATCCAGAGAG Reverse TGCACATTTCCTGTCAAACC	63
mGria2	Forward CAGTTTCGCAGTCACCAATG Reverse ACCCAAAAATCGCATAGACG	65
mGria3	Forward CCACTTGGATTCCTCCAATAGT Reverse GCATACACCCCTCTGGAGAA	72
mGria4	Forward CTGCCAACAGTTTTGCTGTG Reverse AAATGGCAAACACCCCTCTA	66
mGrik1	Forward GATATTTGATTGTTCGCACGAG Reverse GCCCATGAACAAAATCTGCT	61
mGrik2	Forward AGTGCCACCATACCATCCAG Reverse GCTGGCACTTCAGAGACATTC	125
mGrik3	Forward AGGTCACTCATCGTCACCACT Reverse ATCAGACTTGCGGAACATGA	60
mGrik4	Forward GCCATTGAGTATGGCACGAT Reverse TGGTAACGGGAATTTTGGAA	65
mGrik5	Forward CCCCTCAGCTAGCCTCATCT Reverse GCCTCGCACCAGTTCTTCTA	67
mGrin1	Forward CATTTAGGGCTATCACCTCCA Reverse CACTGTGTCTTTTTGGTTTTGC	113
mGrin2a	Forward ATTCAACCAGAGGGGCGTA Reverse TTCAAGACAGCTGCGTCATAG	87
mGrin2b	Forward GGGTTACAACCGGTGCCTA Reverse CTTTGCCGATGGTGAAAGAT	65
mGrin2c	Forward GAAGCGGGCCATAGACCT Reverse TGGCAGATCCCTGAGAGC	90
mGrin2d	Forward TGCGATACAACCAGCCAAG Reverse AGATGAAGGCGTCCAGTTTC	72
β-actin	Forward CGTGGGCCGCCCTAGGCACCAG Reverse TTGGCCTTAGGGTTCAGGGGGG	243

Cont.

Supplementary Table 1. (cont.)

Genes	Primer Sequences	Product Sizes (bp)
hGRIA1	Forward CAGCGACAGCTTTGAGATGA Reverse GATGGCATAGACTCCTTTGGA	64
hGRIA2	Forward TGTGGAGCCAAGGACTCTG Reverse CCCCCGACAAGGATGTAGA	89
hGRIA3	Forward GGAGACTGCTTAGCAAATCCTG Reverse TCATTCCTTGTACTTGCACCA	88
hGRIA4	Forward CCAAACAAACAGAAATTGCCTA Reverse CCACATCTTTTCATACACTGCTATTT	66
hGRIK1	Forward GCGGTTAGAGATGGATCAACA Reverse TCATGAAAGCCCACATCTTCT	79
hGRIK2	Forward CACCCTTGCAACCCTGAC Reverse TTTGGGCATGAGCTCAGAA	111
hGRIK3	Forward GAGTATGGGGCTGTCAAGGA Reverse CGAAGGTGGAGATCTTGGAT	67
hGRIK4	Forward CAAGGAGGAAGATCACAGAGC Reverse TGGTAACGGGAATTTTGGAA	87
hGRIK5	Forward TTGGCGAGCTCATCAACC Reverse TGACCTTCTCCCGCTCAG	75
hGRIN1	Forward TACAAGCGGCACAAGGATG Reverse TCAGGCTCTGCTCTACCACTC	110
hGRIN2A	Forward CTTGGAAGAGGCAGATCGAC Reverse CTTCTCGTTGTGGCAGATCC	104
hGRIN2B	Forward AGCAATGGGACTGTCTCACC Reverse AACATCATCACCCATACGTCAG	68
hGRIN3A	Forward AAATCCAAGCTGCAATACTGG Reverse AAATGCTGCTGCTTTTCCTC	89
hGRIN3B	Forward ACTGCTGACCGTGGGAAA Reverse ATGAACTCGGACAGGTTGGA	93
hSLC17A7	Forward ACGACAGCCTTTTGTGGTTC Reverse TGAGGGGGTTCATGAGTTTC	243
hGAD1	Forward CCAACAGCCTGGAAGAGAAG Reverse GGTGGAGCGATCAAATGTCT	247
hTH	Forward ACTGGTTCACGGTGGAGTTC Reverse AGCTCCTGAGCTTGTCCTTG	230
hDLG4	Forward CCGACAAGTTTGGATCCTGT Reverse CCCATAGAGGTGGCTGTTGT	163
hMAP2	Forward CCAATGGATTCCCATACAGG Reverse CTGCTACAGCCTCAGCAGTG	179
hENOLASE2	Forward ACTTTGTCAGGGACTATCCTGTG Reverse TCCCTACATTGGCTGTGAACT	93
hGAP43	Forward GAGGATGCTGCTGCCAAG Reverse GGCACTTTCCTTAGGTTTGGT	111
hGADPH	Forward CTCTGCTCCTCCTGTTCGAC Reverse GCCCAATACGACCAAATCC	119